Oculocerebrorenal Syndrome: Case Report with CT and MR Correlates

Lorcan A. O'Tuama[1] and D. Wayne Laster

We report a detailed imaging investigation of the oculocerebrorenal syndrome (OCRS), or Lowe's syndrome. Our study includes the first detailed account of the cranial CT features, as well as the first MR imaging observations. A combination of soft-tissue and bony abnormalities may allow a specific radiographic separation of this disorder from other diseases causing the CT appearance of leukoencephalopathy. Also, the radiographic features cast new light on the neuropathologic basis of OCRS.

Case Report

A 3½-year-old boy presented for cranial CT because of profound developmental delay and recurrent seizures. He was the 3.6-kg product of a full-term gestation, complicated by breech presentation requiring cesarean section. Delivery took place through meconium-stained liquor, and low Apgar scores were noted. By 2½ months, bilateral cataracts with congenital glaucoma, hypotonia, and severe developmental delay were evident. Generalized and partial seizures began at 4 months and continued despite phenobarbital treatment. Multiple long-bone fractures also occurred within the first year of life. A diagnosis of OCRS was made in early infancy. Family history was negative for cancer, renal disease, epilepsy, and congenital defects. Physical examination showed a youngster with marked developmental delay and growth retardation (weight 8.2 kg [<5%], height 81.3 cm [<5%], head circumference 37.5 cm [<5%]). Severe visual impairment with congenital glaucoma of the left eye and bilateral iridectomies were seen. Frontal bossing was evident. Nystagmus was present on right lateral and downward gaze. Limb deformity secondary to multiple long-bone fractures was impressive. Biochemical abnormalities included proteinuria and generalized aminoaciduria. Bone radiographs showed prominent rachitic changes including bone resorption, splaying and cuffing of the metaphyses, and deformities from healed fractures. These features were typified by radiographs of the right shoulder, wrist, distal radius and ulna, femur, and tibia. All radiographic abnormalities showed interval progression from 3 years earlier. Skull radiographs showed prominent convolutional markings in the occipital region. CT (GE 8800 scanner) showed diffuse scalloping of the calvarial bones, including the regions of the upper convexity. Irregular areas of abnormal lucency were seen in the white matter surrounding the frontal horns and body of the lateral ventricles and extending into the parietooccipital association fibers (Fig. 1A). These changes showed slight hemispheric asymmetry but were confluent and homogeneous.

The patient was examined with a Picker International 1000 prototype MR resistive imager operating at 0.15 T and a frequency of 6.4 mHz. Sixteen contiguous 10-mm-thick images were obtained using spin-echo techniques to obtain T2-weighted images (TE = 80 msec, TR = 3000 msec) and T1-weighted images (TE = 40 msec, TR = 800 msec). The findings on the T2-weighted images showed white CSF, which is normal at this pulse sequence. The abnormal areas of bright signal intensity were similar to those changes seen in demyelinating disease, such as multiple sclerosis. These changes were patchy, in contrast to the confluent abnormality seen with CT. The T1-weighted images failed to show either abnormal high or low signal areas in the white matter (Fig. 1B). However, this finding may have been influenced by the inherent T2-dependent component of the nominally T1-weighted image.

Discussion

Our patient conforms to the clinical and biochemical phenotype of the "oculocerebrorenal syndrome." Since they were first described [1–3], ocular abnormalities (including cataracts in infancy), followed by progressive neurologic deterioration, have been consistently recognized. A characteristic defect in renal tubular transport causes an aminoaciduria, especially for basic amino acids and cystine [4].

Previous CT literature [5] contains only brief and incidental reference to the findings in OCRS. We have found no publication of MR features. This report presents the first detailed report of CT findings in OCRS and includes the first published MR data.

CT showed striking abnormalities on the images derived from both bone and brain windows. Marked scalloping of the calvarial bones was seen especially in the occipital regions. The appearance had some similarity to Lückenschädel. However, the patient's age effectively excludes consideration of this condition. Furthermore, the features of type II Chiari malformation, often associated with Lückenschädel, were absent. Calvarial deformity may also be caused by craniosynostosis [6]. Our patient showed no direct radiographic evidence of craniosynostosis, and commonly associated abnor-

Received March 20, 1985; accepted after revision August 6, 1985.

[1] Both authors: Department of Radiology, The Bowman Gray School of Medicine of Wake Forest University, 300 South Hawthorne Rd., Winston-Salem, NC 27103. Address reprint requests to D. W. Laster.

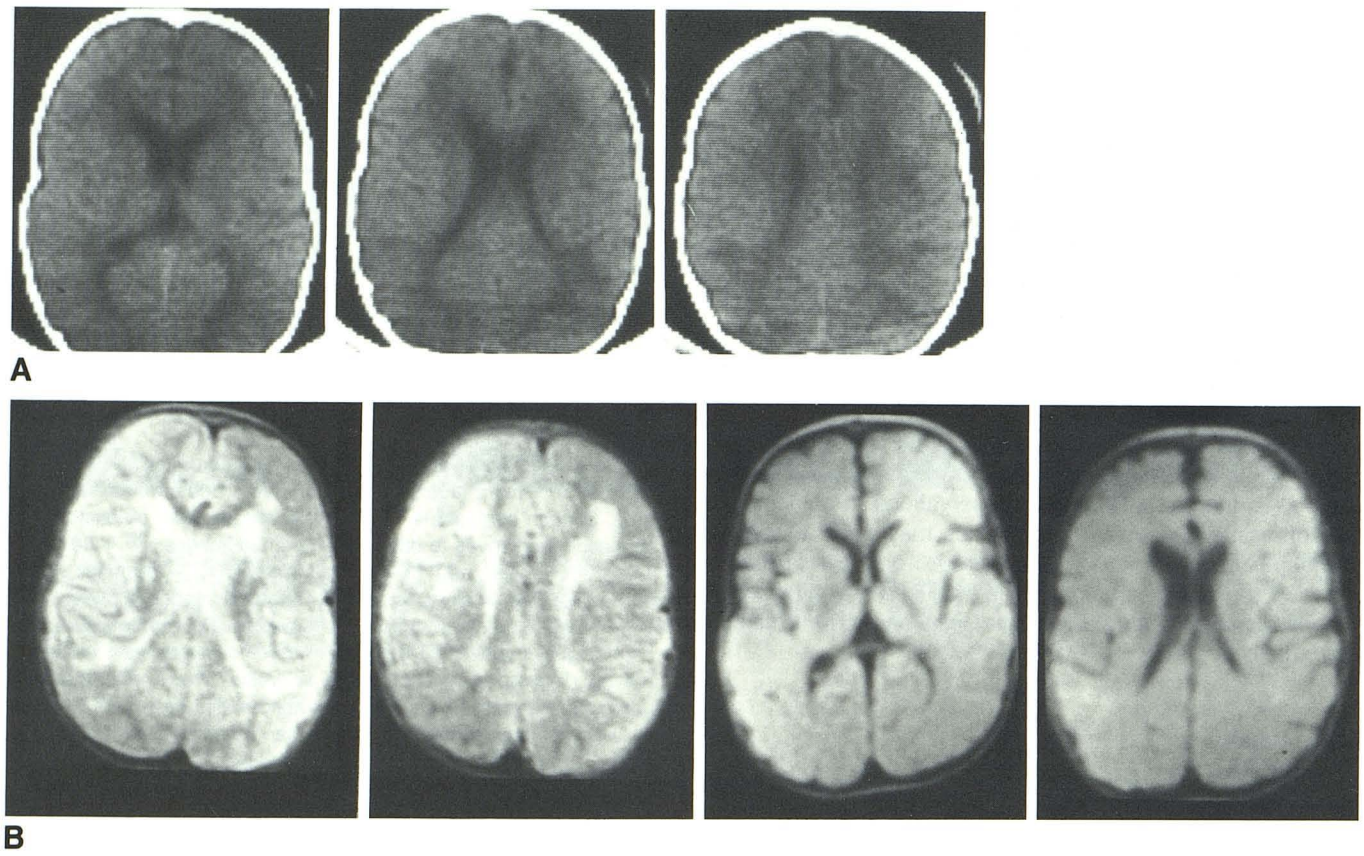

Fig. 1.—*A*, Contiguous uninfused CT images show prominent periventricular white-matter lucency and increased convolutional markings.
***B*, Top row: Contiguous 10-mm-thick T2-weighted MR images (TE = 80 msec, TR = 3000 msec). Patchy, irregular, round, abnormal areas of high signal intensity are present in periventricular white matter. Bottom row: Contiguous 10-mm-thick slightly T1-weighted MR images (TE = 40 msec, TR = 800 msec) fail to show abnormal signal from white matter. (See discussion in text.)**

malities of the petrous-sphenoid angle and brain abnormalities were absent.

The soft-tissue CT abnormalities comprised mild, generalized ventricular dilatation with extensive periventricular decrease in density. The sulci over the upper cerebral convexities appeared normal, and there was no disproportionate enlargement of the temporal horns. These changes show no major distinguishing features from those described in a wide variety of other leukoencephalopathies, such as multiple sclerosis [7], progressive multifocal leukoencephalopathy [8], and metachromatic leukodystrophy [9]. None of these conditions, however, shows the calvarial abnormalities we have found in OCRS.

The marked calvarial changes, which extended into the upper cranial vault, clearly exceeded the milder degrees of bone scalloping sometimes seen in normal children. Our patient did not show other clinical features, such as prolonged recumbency in infancy or sudden growth acceleration, that might modify calvarial growth. Increased convolutional impressions are of further interest in a patient whose presumed reduced brain growth would predict the opposite abnormality of skull development. Thus, the calvarial changes of OCRS cannot be explained, at least in the present case, as a secondary phenomenon. These features may aid in radiologic differentiation of this disorder from other conditions causing decreased white-matter density. Without pathologic material, which is not available at this time, the significance of the MR findings is not known, except that these lesions represent an increase in the T2 relaxation time.

Striking variability prevails in published reports of the neuropathologic features of OCRS. Cerebral malformations (e.g., smallness of the superior temporal gyri, splenium, and medical lemnisci) are noted by some authors [10] but not by others [3, 11, 12]. Some [13] have even failed to find consistently specific neuropathologic abnormalities. Thus, extant reports fail to provide a consistent morphologic basis for a disorder that shows the clear clinical behavior of a progressive metabolic encephalopathy. In the case of other leukoencephalopathies [14], CT abnormalities correlate closely with the existence and even the detailed anatomic distribution of the underlying neuropathologic findings. Thus, the detailed imaging characteristics of OCRS reported here are important in validating and categorizing its neuropathologic place among the leukodystrophies.

REFERENCES

1. Lowe CU, Terrey M, MacLachlan EA. Organic-aciduria, decreased renal ammonia production, hydrophthalmos, and mental retardation. *Am J Dis Child* **1952**;83:164–184

2. McCance RA, Matheson WJ, Gresham GA, Elkinton JR. The cerebro-oculararrenal dystrophies: a new variant. *Arch Dis Child* **1960**;35:240–244
3. Chutorian A, Rowland LP. Lowe's syndrome. *Neurology* **1966**;16:115–122
4. Tripathi RC, Cibis GW, Tripathi BJ. Symposium in ocular pathology. Lowe's syndrome. *Trans Ophthal Soc UK* **1980**;100:132–139
5. Di Chiro G, Arimitsu T, Brooks RA, et al. Computed tomographic profiles of periventricular hypodensity in hydrocephalus and leukoencephalopathy. *Radiology* **1979**;130:661–666
6. Carmel PW, Lucken MG, Ascherl GF. Computed tomographic evaluation of skull base and calvarial deformities and associated intracranial changes. *Neurosurgery* **1981**;9:366–372
7. Gyldensted C. Computed tomography of the brain in multiple sclerosis. A radiological study of the brain in 110 patients with special reference to demonstration of cerebral plaques. *Acta Neurol Scand* **1976**;53:386–389
8. Bosch EP, Cancilla PA, Cornell SH. Computed tomography in progressive multifocal leukoencephalopathy. *Arch Neurol* **1976**;33:216–224
9. Arimitsu T, Di Chiro G, Brooks RA, Smith PB. White-gray matter differentiation in computed tomography. *J Comput Assist Tomogr* **1977**;1:437–442
10. Malin MA, Sylvester PE. Clinicopathological studies of oculocerebrorenal syndrome of Lowe, Terry and MacLachlan. *J Ment Defic Res* **1980**;24:1–16
11. Guazzi GC. Neurologie et neuropathologie du syndrome de Lowe. *J Neurol Sci* **1966**;3:353–373
12. Garzuly F, Jellinger K, Szabo L, Toth K. Morbid changes in Lowe's oculocerebrorenal syndrome. *Neuropädiatrie* **1973**;4:304–313
13. Bannerjee AK, Allen IV, McKee P. Oculocerebrorenal syndrome: failure to demonstrate specific neuropathological abnormalities in four cases. *Ir J Med Sci* **1982**;151:42–45
14. Valvoris A, Schuliger O, Hayek J. Computed tomography in "nonketotic hyperglycinemia." *J Comput Assist Tomogr* **1981**;4:265–270